

A HIGH-POWER, HIGH-REPETITION RATE THz SOURCE FOR LCLS-II PUMP-PROBE EXPERIMENTS*

Z. Zhang, A. S. Fisher, M. C. Hoffmann, Z. Huang[†], B. Jacobson,
 P. S. Kirchmann, W.-S. Lee, A. Lindenberg, E. Nanni, R. Schoenlein
 SLAC National Accelerator Laboratory, Menlo Park, CA, USA
 S. Sasaki, J. Xu, Argonne National Laboratory, Lemont, IL, USA

Abstract

Experiments using a THz pump and an x-ray probe at an x-ray free-electron laser (XFEL) facility like LCLS-II require frequency-tunable (3 to 20 THz), narrow bandwidth (~10%), carrier-envelope-phase-stable THz pulses that produce high fields (> 1MV/cm) at the repetition rate of the x rays and well synchronized with them. In this paper, we study a two-bunch scheme to generate THz radiation at LCLS-II. We describe the two-bunch beam dynamics, the THz wiggler and radiation, as well as the transport system bringing the THz pulses from the wiggler to the experimental hall.

INTRODUCTION

The effective coupling of advanced THz sources with XFEL capabilities will open many new science opportunities. THz oriented workshops at SLAC [1], FERMI, Eu-XFEL [2] and elsewhere in the past eight years have highlighted the demand for the ability to carry out these types of experiments.

The new science opportunities presented by a high-repetition rate FEL such as the LCLS-II create new opportunities, demands, and challenges for THz sources that go beyond what has been considered in previous workshops. Some critical capability gaps can already be identified that appear to be beyond the projected achievable properties of table-top sources. Among them are the intense sources in the well-known THz gap between 3-15 THz. For field driven effects, a broadband, single-cycle THz pulse with a peak electric field strength of 10 MV/cm can approach the atomic bonding strength in matters. For resonant excitation, a tunable, narrow bandwidth (~ 10%) source with at least 10 μ J pulse energies are desired. These required THz characteristics are summarized in Table 1.

Table 1: Required THz Characteristics

| Waveform | Single cycle | | 10 cycles | |
|----------------|--------------|-------------|-------------|-------------|
| | E-field | 10 MV/m | | 1 MV/m |
| Frequency | 5 THz | 15 THz | 5 THz | 15 THz |
| Spot Size | 200 μ m | 100 μ m | 200 μ m | 100 μ m |
| Pulse Duration | 100 fs | 33 fs | 1000 fs | 330 fs |

Although a dedicated accelerator with tens of MeV beam energy can achieve some of these capabilities [3, 4], it becomes increasingly difficult to reach 10 THz and higher

* Work supported by U.S. Department of Energy Contracts No. DE-AC02-76SF00515.

[†] zrh@slac.stanford.edu

frequencies with significant pulse energies. In addition, a high-repetition rate stand-alone accelerator with the technical issues of synchronization and the associated machine protections becomes rather complex. Inspired by the pioneering work of the FLASH THz beamline [5], we propose to install a permanent-magnet or electromagnet wiggler after the LCLS-II undulators and to use a two-bunch scheme to produce intense THz pulses for high-rep rate pump-probe experiments. We note that an earlier study of a THz source for Eu-XFEL has a similar two-bunch scheme while employing a high-field superconducting wiggler [6].

TWO-BUNCH SCHEME

Figure 1 shows a schematic of the two-bunch concept at LCLS-II to produce intense THz radiation. Both bunches are generated by the LCLS-II injector with suitable time separation (~110 ns). Because the THz pump must arrive before the X-ray probe, a first bunch is used to produce THz in the wiggler and a second bunch is for FEL lasing. In our design, the THz bunch will be accelerated to 4 GeV and then kicked out to the bypass line. For THz generation, a higher bunch charge and a shorter bunch length are always desirable. The beam parameters of the THz bunch will be optimized to cover the frequency range from 3 to 20 THz. Moreover, stronger compression of the THz bunch results in poorer beam quality and hence suppress its FEL lasing in the SXR undulator.

The accelerator settings of the LCLS-II are optimized to deliver electron bunches for FEL lasing. The control of the THz bunch cannot be allowed to alter the beam dynamics of the FEL bunch. The compression of the THz bunch can be adjusted by the laser injection time, which changes the acceleration phase in the SRF linac (L1) before the first magnetic chicane (BC1). Figure 2 shows that offsetting the laser injection time changes the beam arrival time of 200-pC bunch at the start of L1. The simulations were performed with ASTRA [7]. The change of arrival time at the start of the L1 varies the beam energy chirp and beam compression downstream. An earlier laser pulse shortens the first bunch for better THz generation. Figure 3 shows the final RMS bunch length at the undulator entrance for the 200-pC THz bunch at different offsets of the relative laser injection time.

Figure 4 shows the bunching factors of the THz beam (100 pC and 200 pC) at different frequencies. The bunching factor of the 200-pC bunch damps quickly with increasing frequency. In practice, we can optimize the bunch charge

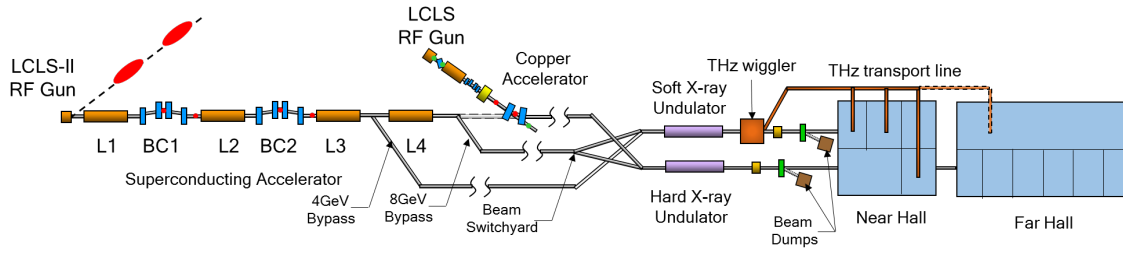


Figure 1: LCLS-II layout showing the linac, soft and hard x-ray undulators, the proposed THz wiggler and transport line, and the Near and Far Experimental Halls.

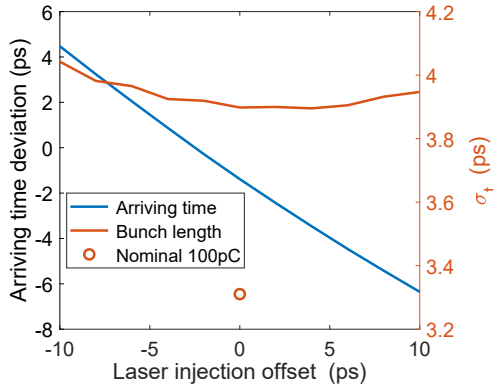


Figure 2: The change in arrival time and RMS bunch length of a 200-pC THz bunch for various laser injection timing offsets at the start of L1 compared with the nominal 100-pC FEL beam. A negative time means arriving the laser pulse arrives earlier in its RF period than does the laser pulse for a nominal 100-pC bunch.

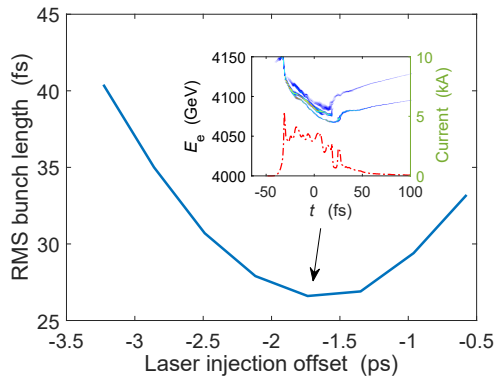


Figure 3: RMS bunch length of the 200-pC THz bunch at the undulator entrance for different laser injection time offset. Insert shows the simulated longitudinal phase space (blue) and the projected peak current (red) for the -1.7 ps laser injection time offset.

to produce THz pulses with high radiated energy at any frequency in the 3- to 20-THz range.

THz WIGGLER AND RADIATION

The parameters of the THz wiggler are optimized for a 4-GeV electron beam energy. We choose 10 wiggler periods to

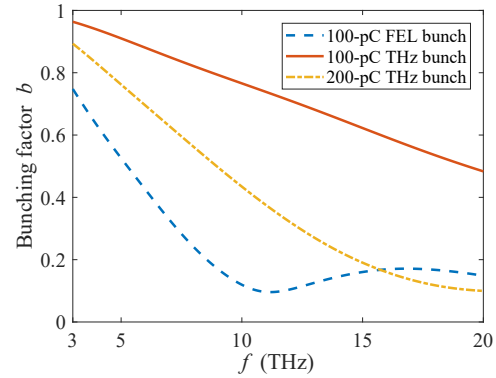


Figure 4: Bunching factors of the nominal LCLS-II 100-pC FEL bunch and the 200-pC THz bunch for 3~20 THz.

produce THz radiation with 10% bandwidth. Figure 5 shows the required peak magnetic field for different wiggler periods. The main limitation in practice is the available magnetic field with a reasonable wiggler gap. We consider two wiggler technologies for THz generation, based on hybrid permanent magnets and electromagnets.

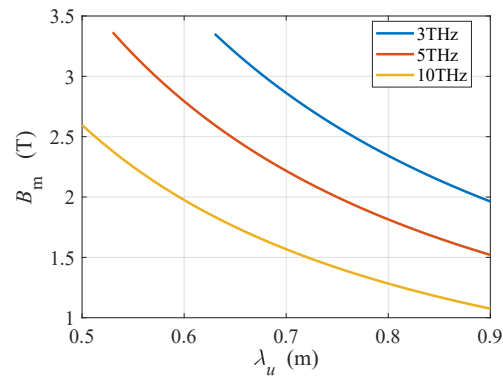


Figure 5: Magnetic field at different wiggler periods when using 4 GeV beam to generate 3, 5 and 10 THz radiation.

In a hybrid permanent-magnet wiggler, the peak field can be numerically fitted as a function of gap g and period λ_u [8]

$$B_0 = a \exp \left(b \frac{g}{\lambda_u} + c \left(\frac{g}{\lambda_u} \right)^2 \right) \quad (1)$$

with $a = 3.381$, $b = -4.730$, $c = 1.198$. Based on this, the wiggler gap is shown in Fig. 6. Note that the equation is

Content from this work may be used under the terms of the CC BY 3.0 licence (© 2019). Any distribution of this work must maintain attribution to the author(s), title of the work, publisher, and DOI

valid in the range $0.1 < g/\lambda_u < 1$. When $\lambda_u = 0.77$ m, the required wiggler gap is ~ 50 mm at 3 THz.

In an electromagnet wiggler, the gap is fixed and the magnetic field is varied by the current in the coils. The conventional electromagnet can reach 2.5 T with a clearance gap of 50 mm. In this case, we can produce 3-THz radiation when the wiggler period is 78 cm. An additional advantage of the electromagnet wiggler is that the magnetic field can be independently controlled by separate power supplies.

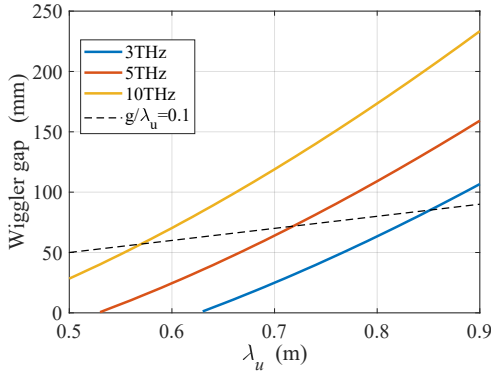


Figure 6: Gap of hybrid-type permanent magnetic wiggler at different wiggler period when using 4 GeV beam to generate 3, 5 and 10 THz radiation.

The transverse distribution can be calculated from angular distribution of undulator radiation. The long wiggler length and small gap limit the THz output due to diffraction, especially at low frequency. Figure 7 shows the transverse distribution of the radiation at 10 THz (with 10% bandwidth from 9.5 to 10.5 THz) for the 77-cm wiggler period. We also present the energy density profiles along the two axis. It can be seen that most of the radiation is emitted within a ~ 4 mrad angle. The collection angle in the wiggler can be estimated by $\theta = g/L_u$ where $L_u = N_u \lambda_u$ is the total wiggler length. With a 50-mm gap in a 10-period wiggler, $\theta = 6.5$ mrad, which is larger than the angular divergence of the 10-THz radiation.

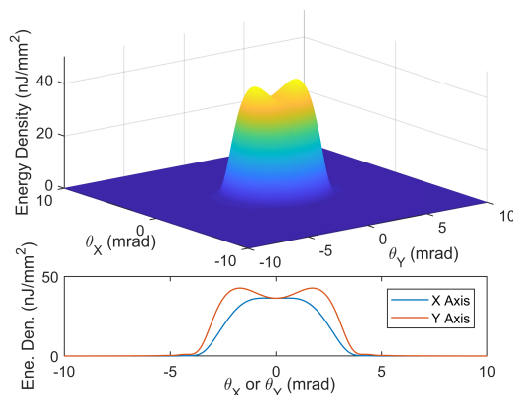


Figure 7: Transverse distribution of 10 THz radiation and the corresponding energy density profiles along two axis.

The total achievable THz pulse energy depends on the specific layout of wiggler and transport system (THz mir-

rors). Here we can estimate the pulse energy by the bunching factor spectra and the simplified equation as [9]

$$\frac{dW}{d\omega/\omega} = 1.43 \times 10^{14} N_u I [A] \frac{hK^2 [JJ_h]^2 \text{ photons}}{1 + K^2/2 \text{ 0.1\% BW}} \quad (2)$$

The pulse energy from the 100-pC and 200-pC THz beam in Fig. 4 is presented in Fig. 8.

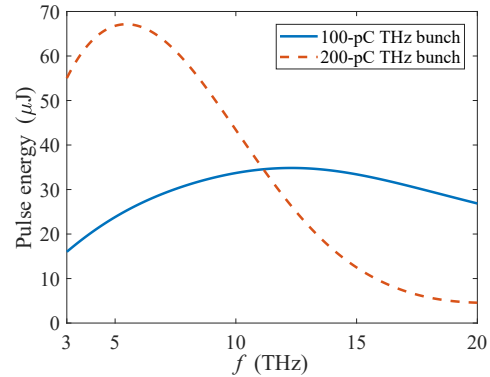


Figure 8: The estimated THz energy of the 100-pC and 200-pC THz bunch for at different radiation frequency.

THz TRANSPORT

Soft X-rays follow a nearly straight path from the undulator to the user hutches in the Near Experimental Hall. The strongly diffracting THz requires optical relay imaging through large-diameter tubing (200 mm) with frequent reimaging (every 12 to 15 m). The imaging uses reflective optics, due to the wide bandwidth and the lack of good refractive materials. Either off-axis paraboloidal (OAP) or toroidal mirrors may be used, with 45° incidence. Imaging is maintained by separating adjacent mirrors by a distance equal to the sum of their focal lengths. Since water vapor absorbs THz, the tubing should be evacuated to 1 Pa or below. Alternatively, the tubing could be filled with nitrogen or another inert gas. A preliminary layout requires a combination of 12 focusing and 22 flat mirrors to reach one of the principal hutches. Fortunately, reflection losses at this frequency are below 1% per surface, which would provide 70% transmission. The time between the two electron bunches is determined by the extra path of the THz compared to the straight x-ray path. The path through the maze requires an additional 108 ns.

REFERENCES

- [1] K. Gaffney, J. Goldstein, P. Kirchmann, A. Lindenberg, and Z.-X. Shen, Workshop *Frontiers of THz Science*, (2012).
- [2] P. Zalden *et al.*, Terahertz Science at European XFEL, XFEL.EU TN-2018-001-01.0 (2018).
- [3] B. Green *et al.*, *Nature Sci. Rep.*, vol. 6, 22256 (2016), doi: 10.1038/srep22256(2016).
- [4] J. Schmerge *et al.*, SLAC-R-1049 (2013).

- [5] K. Tiedtke *et al.*, *New Journal of Physics*, vol. 11, 023029 (2009), doi:10.1088/1367-2630/11/2/023029.
- [6] T. Tanikawaa *et al.*, *Journal of Inst.*, vol. 14, P05024 (2019), doi:10.1088/1748-0221/14/05/p05024.
- [7] K. Floettmann, A Space Charge Tracking Algorithm, <http://www.desy.de/~mpyflo/>.
- [8] K. Halbach, *Nucl. Instrum. Methods*, vol. 187, 109 (1981), doi:10.1016/0029-554X(81)90477-8.
- [9] K.-J. Kim, Z. Huang, R. Lindberg, *Synchrotron Radiation and Free-Electron Lasers*, Cambridge University Press, 2017, doi:10.1017/9781316677377.003.